Journal of Food Measurement and Characterization (2022) 16:2154–2171
https://doi.org/10.1007/s11694-022-01335-z

ORIGINAL PAPER

Bioaccessibility of total phenolics and antioxidant activity of melon slices dried in a heat pump drying system

Azime Özkan Karabacak[1] · Cüneyt Tunçkal[2] · Canan Ece Tamer[1] · Ömer Utku Çopur[1,3] · Perihan Yolci Ömeroğlu[1,3]

Received: 25 September 2021 / Accepted: 30 January 2022 / Published online: 20 February 2022

Abstract

For drying of heat-sensitive crops at low temperature and humidity, heat pump drying (HPD) could be a useful option. The aim of this study was to investigate the effect of HDP process conditions on total phenolic content (TPC), antioxidant activity (AA) and their in-vitro bioaccessibility of the melon slices and to optimize HPD conditions to obtain dried product with high bioactive properties. Drying air temperature (35–45 °C), air velocity (5–9 m/s) and slice thickness (0.5–1 mm) were selected as variables for Box-Behnken experimental design. Depending on the stability of the phenolics, physical changes of the matrix, and the HPD conditions, both incremental (2–114.39%) and decremental (5–47%) effects of drying were observed for AA and TPC of the melon slices. After in vitro *digestion,* dried melon slice was found to contain higher amounts of bioaccessible total phenolics (up to 165%) and AA measured by DPPH assay (up to 188.19%) compared to fresh melon slices, on the other hand bioaccessibility of AA by CUPRAC and FRAP assays after digestion decreased (up to 63%) by drying process. The relation between the responses (AA, TPC and their in-vitro bioaccessibility) and the variables were best fitted to quadratic, reduced quadratic and reduced cubic models with high R^2 values by response surface methodology. The optimal condition for all responses with composite desirability of 0.777 was: 35 °C drying air temperature, 0.5 m/s drying air velocity and 9 mm slice thickness. Melon slices dried by HPD could be accepted as an innovative snack for health-conscious consumers.

Keywords Melon · Heat pump drying · Bioavailability · Phenolics · Antioxidant capacity

Introduction

Melon (*Cucumis melo* L.) is a fruit consumed all around the world, especially in tropic countries [1]. Fruits are mainly consumed in raw or freshly cut forms, morever their dried, canned in syrup, juice, nectar, compote or jam forms are commonly preferred [2, 3]. In addition to carbohydrates, proteins and vitamins (A, B_1, B_2, B_3, B_6, C, K), melon encloses antioxidant compounds like phenolics and carotenoids [4, 5]. Fresh melon is highly perishable, therefore drying can be used as a tool to extend its shelf life, to raise its potential utilization and to draw advantage from its potential health promoting benefits and added value [6, 7]. On the other hand, it has been known that the processing of fruits and vegetables affects their quality, phenolic content and antioxidant properties [8]. It has been reported that drying process conducted with or without pre-treatments including ultrasound, vacuum, and osmotic drying could dramatically affect the quality characteristics of the melon, comprising color and texture and cause a reduction in bioactive compounds [9]. Sabovics et al. [10] indicated that the fruit variety, in addition to the drying method had a substantial effect on total phenolics (TP) and antioxidant activity (AA) of the melon. Depending on the potentiality of oxidative decomposition either enzymatically or by pyrolysis of polyphenols, drying processes is usually considered as unfavorable [11]. Therefore, alternative to the conventional drying methods has been sought for heat sensible foods.

Heat pump-assisted dryers (HPD) are well known cost-competitive equipments, and extremely useful in drying of heat-sensitive materials at low temperature and humidity [12]. Erbay and Icier [13] successfully utilized HPD for

✉ Canan Ece Tamer
etamer@uludag.edu.tr

[1] Department of Food Engineering, Faculty of Agriculture, Bursa Uludag University, 16059 Gorukle, Bursa, Turkey

[2] Electric and Energy Department, Air Conditioning and Refrigeration Technology Program, Yalova Community College, Yalova University, 77100 Yalova, Turkey

[3] Science and Technology Application and Research Center, Bursa Uludag University, 16059 Gorukle, Bursa, Turkey

drying of olive leaves. Ong and Law [14] utilized a closed-loop single-stage HPD for drying of salak fruit. Positive results were acquired in terms of higher TPC, higher ascorbic acid content, better storage stability, and the lowest total color change under the HPD. In order to obtain high quality products by minimizing undesirable changes in the the fruit during drying, optimization of the process conditions of HPD is essential. Response Surface Methodology (RSM) could be used in order to determine the effects of the different process variables that have an effect on the final product [15]. Several researchers have used RSM for optimization of drying process (i.e. convective drying, combined microwave and hot air drying, vacuum drying, spray drying, infrared drying, convective-infrared drying, electrohydrodynamic drying) of fruits (i.e. red currant, pink guava, white mulberry, apple, kiwi fruit) and vegetables (turnip, purple cabbage, cauliflower, eggplant) [16–24]. Tunckal et al. [25] optimized the HPD process conditions (in terms of air temperature, air velocity and slice thickness) for melon slices with RSM to get minimum specific energy consumption and maximum moisture diffusivity.

Several studies conducted for dried fruits have been focused on bioaccessibility, which is the portion of a compound that is released from food matrix in the GI tract and becomes available for the absorption into intestinal epithelium cells [11, 26–32]. The reported studies on bioaccessibility mimiced the GI conditions and determined the fraction of a specific compound available for absorption. While in vitro digestion models are fast and reliable, in vivo methods have ethical constraints [33]. However, to the best of authors' knowledge, the optimization of closed loop HPD process conditions (in terms of air temperature, air velocity and slice thickness) has not been studied to achieve dried melon slices with high in vitro bioaccessibility and antioxidant activity. In the light of the reported studies in literature, the objective of this research was to study the effect of the HPD process conditions on total phenolic content (TPC), antioxidant activity (AA) and their in-vitro bioaccessibility for the melon slices as a healthy snack. Consequently, it was aimed to optimize the process conditions in terms of air temperature, air velocity and slice thickness by RSM to obtain dried product with high bioactive properties.

Materials and methods

Materials

Fresh melons (Futuro F1) were purchased from a local producer in Yalova, Turkey at the biologically ripened stage. Prior to experimental trials, the melons were washed with tap water, peeled and sliced into 5 mm-thick, 7 mm- thick and 9 mm- thick slices. The initial moisture content of melon slices was measured with an oven set at 105 ± 3 °C as 7.675 ± 0.85 kg water/kg dry matter (d.b.).

Drying system procedure

Melon slices were dried with a heat pump dryer whose technical properties and detailed schematic diagram were given before by [34]. The dryer was ran for about 30 min to stabilize the drying conditions before the drying process was started. The process input variables included air temperature (35, 40 and 45 °C), air velocity (0.5 m/s, 0.75 m/s, and 1.0 m/s) and slice thickness (5, 7 and 9 mm), respectively. After stabilization of the system, melon slices (635 g) were homogeneously placed on the drying tray. During drying process, the mass loss of samples was monitored by using the load cell at every 4 min and all data were recorded by a computer connected to the system. The temperature and relative humidity of air within the drying system were measured every 1 min by a data collector. When the moisture content of the melon slices decreased about $8 \pm 0.5\%$ (wet basis), the drying procedure was finished. Drying system operates with ± 0.8 °C sensitivity by a digital thermostatic control.

Analysis methods

Chemical extraction of samples from undigessed samples

Melon samples were extracted using the method described by Kamiloglu and Capanoglu [35]. 5 mL of extraction solution (75% aqueous methanol containing 0.1% formic acid) was added to 2.00 ± 0.05 g of sample and kept in a cooled ultrasonic water bath (Bandelin Sonorex RK 510 H, Germany) for 15 min. The samples were then centrifuged (Sigma 3 K 30, Germany) at 2700 g at 4 °C for 10 min and the supernatants were collected. Another 5 mL of extraction solution was added to the pellet and this process was repeated three more times. All four supernatants were combined and adjusted to a final volume of 20 mL. Prepared extracts stored at − 20 °C until analysis.

Spectrophotometric assays

Total phenolic content (TPC) and antioxidant acitivity (AA) were determined using an ultraviolet–visible spectrophotometer (UV-1800, Shimadzu).

TPC analysis was performed according to the spectrophotometric Folin-Ciocalteu method [36]. 0.5 mL of extract was mixed with 0.5 mL of Folin-Ciocalteu (diluted 3 times with water) reagent. After 5 min, 1 mL of saturated sodium carbonate solution (35%) was added to the mixture, vortexed and diluted to 3 mL with 1 mL of distilled water. Subsequently, the diluent was kept in the dark for 30 min, the absorbance was read with the spectrophotometer at 700 nm.

A multi-point lineer calibration curve ($R^2 = 0.9992$) was constructed with standard gallic acid solutions with concentrations ranging between 5 and 50 ppm. The results were calculated from the lineer function of the curve and expressed as mg gallic acid equivalent (GAE)/100 g dry matter.

AA was determined based on 2,2-diphenyl-1-picrylhydrazyl-hydrate (DPPH), Cupric Reducing Antioxidant Capacity (CUPRAC) and Ferric Reducing Antioxidant Power (FRAP) assay methods. In the DPPH assay, 0.1 mL sample extract was mixed with 3.9 mL of (DPPH) solution and vortexed (Vortex Mixer Classic, Velp Scientifca, Italy) for 30 s. Test tubes were kept in the dark at ambient temperature for 30 min. A trolox calibration curve ($R^2 = 0.9997$) was obtained by measuring the reduction in absorbance of the DPPH solution in the presence of different concentrations of trolox (10–100 µmol/L) [37]. In the CUPRAC assay, 100 µL of the sample extract was added to 900 µL of distilled H_2O and CUPRAC reagent which was prepared with the equal amounts of $CuCl_2$, neocuproine, and ammonium acetate solutions, and the absorbance of the sample was measured at 450 nm after 30 min ($R^2 = 0.9933$) [38]. Results were expressed as µmol trolox equivalent (TE)/g dry weight (dw). In FRAP assay, 3 mL of daily prepared FRAP reagent was mixed with 300 µL of distilled water and 100 µL of the sample or blank. The test samples and blank were incubated at 37 °C for 30 min then absorbance was determined immediately at 595 nm. The results were calculated from calibration curve as µmol trolox equivalent (TE)/g dw ($R^2 = 0.9934$) [39].

In vitro gastrointestinal (GI) digestion assay

In vitro GI digestion of the samples was carried out according to the method of Minekus et al. [40], with minor modifications. Samples were passed through a two step GI digestion stage representing the aliquots of the stomach phase and intestinal phase. As reported by Minekus et al. [40], simulated gastric fluid (SGF) and simulated intestinal fluid (SIF) were prepared. The samples were combined with the SGF, porcine pepsin solution (25,000 U/mL, Sigma-Aldrich P6887; USA), and calcium chloride during the gastric phase. The pH of the mixture was then adjusted to 3 with hydrochloric acid, and incubated at 37 °C for 2 h in a shaking water bath (Memmert SV 1422, Memmert GmbH & Co., Germany), and afterwards, 4 mL aliquots were collected for each sample. In order to simulate intestinal digestion, the remainder of the mixture was mixed with the SIF solution, pancreatin solution (800 U/mL, Sigma Aldrich P3292), and bile solution (160 mM), one-by-one. The pH was adjusted to 7.0 with sodium hydroxide, and the samples were incubated at 37 °C for 2 h in a shaking water bath. Subsequently, the samples were centrifuged at 3500 rpm for 10 min, filtered, and the supernatant was collected. After that, the extracts were kept at –20 °C until analyzed. The supernatants were assayed spectrophotometrically for TPC and AA as explained above. The % recoveries were given as the ratios of the values determined after intestinal digestion to the values determined for the initial (undigested) values, and then multiplied by 100.

Experimental design

Response Surface Methodology (RSM) was implemented to analyze the effect of independent variables (factors) such as drying air temperature, slice thickness and drying air velocity on the dependent variables (response) which included total phenolic content, antioxidant (DPPH, FRAP and CUPRAC) activity and their in-vitro bioaccessibility for dried melon slices. Box-Behnken design was used for RSM studies, 17 runs were generated with three levels (− 1, 0, 1) of the independent variables, which were determined based on the preliminary studies. 1 represented highest value, 0 represented the optimal value and − 1 represented the lowest value of the variables. Factors, their levels and the experimental design were shown in Tables 1 and 2. Analytical results of the dependent variables were obtained for each run and were statistically examined with Design Expert software (version 13, Stat-Ease, Inc., Minneapolis, USA). The effect of the factors on the individual response was evaluated and described by using a 5% test of significance. The general polynomial model equation was applied to predict the response variables. The equation is given below:

$$Y = \beta_0 + \sum_{i=1}^{3} \beta_i X_i + \sum_{i=1}^{3} \beta_{ii} X_i^2 + \sum_{i=1}^{2} \sum_{j=i+1}^{3} \beta_{ij} X_i X_j + \varepsilon \quad (1)$$

where β_0, β_i, β_{ii} and β_{ij} is intercept, linear, quadratic, and interaction regression terms, and ε is the error. X_i and X_j are the independent variables and Y is predicted response variable in RSM optimization. Three dimensional graphics were constructed to observe the efects of factors on each response visually, and moreover optimum levels for each factor were obtained to get dried melon slices with higher bioactive capacities.

Table 1 Box–Behnken matrix of independent variables used in the RSM design

Variable	Parameter	Levels		
		− 1	0	1
X_1	Drying air temperature (°C)	35	40	45
X_2	Slice thickness (mm)	5	7	9
X_3	Drying air velocity(m/s)	0.5	0.75	1

Table 2 Experimental design

Run number	Drying air temperature (°C)	Slice thickness (mm)	Drying air velocity (m/s)
1	35	5	0.75
2	45	5	0.75
3	35	9	0.75
4	45	9	0.75
5	35	7	0.5
6	45	7	0.5
7	35	7	1
8	45	7	1
9	40	5	0.5
10	40	9	0.5
11	40	5	1
12	40	9	1
13	40	7	0.75
14	40	7	0.75
15	40	7	0.75
16	40	7	0.75
17	40	7	0.75

Statistical analysis

The experiments were planned in a randomized design with three replicates, each sample was analyzed in duplicate. The results were given as mean values ± standard deviation. All results were statistically utilized by ANOVA using the SPSS 15.0 (SPSS Inc., USA). These analyses were at a 5% significant level. Duncan's multiple range test was utilized for the determination of significant differences ($p \leq 0.05$) between means.

Results and discussion

TPC and AA of fresh melon slice and their bioaccessibility

TPC accepted as an indicator for biological value of a fruit which is a substantial characteristic of the melon [4, 41], therefore high amounts of polyphenols are considered as main source for the AA of the melon [42]. TPC (undigested) of the fresh melon samples analyzed within the scope of this study was obtained as 441.49 mg GAE/100 g dw. Ahmed et al. [7] reported TPC of fresh melon (Kırkağaç cv.) sampled from Turkey as 184.84 mg GAE/100 g dw. Since differences in variety of fruit, its maturity, environmental factors, and agricultural processes, in addition to storage conditions and storage period can affect the TPC of the fruits and vegetables [43], the reported TPC values for the fresh melon in the literature [4, 7, 41, 43] varied from our result.

AA of the fresh melon was investigated with three different assay (DPPH, CUPRAC and FRAP) methods (Table 3) and ranged between 5.48 and 9.59 µmol TE/g dw. Higher AA results was obtained with FRAP, followed by DPPH and CUPRAC, respectively. Consistent to our findings, it has been reported in literature that the analytical results obtained from each assay may differ from each other in terms of the reaction mechanism, substrate type, oxidant and target species, reaction conditions and oxidation initiator [44]. In addition, the affinity of the antioxidants to water or lipid phase, namely hydrophilic and lipophilic behaviours, type of the food matrix and the matrix based interferances may affect the AA results [45]. Consequently, it can be stated that determination of the antioxidant capacity of foods using a single assay is not reliable [46, 47]. Şelale et al. [48] indicated that when comparing with other fruits, melon has moderate total water-soluble AA. They reported that fluctuation of total water soluble AA (ABTS assay) of the melons grown in Turkey ranged between 1.18 and 4.64 mmol TE kg^{-1}. However, Bileva et al. [41] mentioned that Galia, Hybrid 15 F1 and Desserten 5 variety melon samples demonstrated the AA evaluated by DPPH method as 5.2, 14.4 and 25.6 mM TE/100 g, respectively. In another study, AA value (DPPH) of fresh melon (Kırkağaç cv.) was determined as 0.15 mmol TE/100 g [49]. The difference between the AA of the melon reported in the literature and in the scope of the current study can be attributed to the variety of the fruits.

Table 3 shows changes in TPC and AA of fresh melon samples during in vitro digestion. In vitro gastric digestion caused a decrease in TPC values for fresh melon compared to the undigested samples, with a recovery of 80.77%. On the other hand, bioaccessibility of TPC in fresh melon samples after intestinal digestion was determined as 149% compared to undigested samples. This result is inline with the

Table 3 The changes in TPC and AA of fresh melon samples during in vitro digestion

	TPC (mg GAE/100 g dw)	DPPH (µmol TE/g dw)	CUPRAC (µmol TE/g dw)	FRAP (µmol TE/g dw)
Undigested	441.49	6.45	5.48	9.59
Simulated gastric digestion	356.61	2.01	3.64	15.78
Simulated intestinal digestion	657.91	1.44	3.25	16.24

results reported by Bhatt and Patel [50] for garlic and also, Pavan et al. [51] for jackfruit whereby the increment in the TPC was attributed to the gradual delivery of polyphenols during the GI digestion. Mosele et al. [52] studied stability of *Arbutus unedo* bioactive compounds under in vitro digestion. They indicated that bioaccessibilities of phenolics and other type of antioxidant compounds varied in vitro gastric and intestinal digestive conditions depending on the type of the food matrix and chemical compositions of the bioactive compounds.

After gastric digestion and intestinal digestion (appr. 2 h each), AA of fresh melons measured using DPPH and CUPRAC assays decreased by 69–78% and 34–40%, respectively. On the other hand, FRAP value increased by 164.55% and 169.34% after gastric and intestinal digestion, respectively compared to undigested samples ($p < 0.05$) with respect to undisgested. Similarly, Gullon et al. [53] indicated increment of FRAP value of pomegranate peel flour in the gastric step as 135% with respect to its initial extract ($p < 0.05$). According to Gullon et al. [53], multiple alterations in phenolics and flavonoids such as (i) modification of chemical structure, (ii) enhanced or attenuated solubility or (iii) interaction with other compounds could have occurred during the progress of the GI digestion of pomegranate peel flour, which influenced their bioaccessibility. Moreover, Lucas-Gonzalez et al. [54] declared that, after gastric phase, the FRAP value increased 24.77% with respect to initial value of maqui berry extracts ($p < 0.05$). Tomas et al. [55] analyzed the changes in total AA of tomato and processed sauce during in vitro GI digestion. While initial value of AA (CUPRAC) of tomato fruit was 109.3 mg TE/100 g fresh weight, AA after in vitro stomache and intestinal phase were 76.8 and 182.1 mg TE/100 g fresh weight, respectively. The change in AA activity was explained by the effect of intestinal digestive enzymes on the complicated food matrix, catalyzing the delivery of bound phenolics [56].

Effect of drying on TPC, AA and their bioaccessibility

The effect of drying conditions and in vitro digestion on the TPC and AA measured by DPPH, CUPRAC and FRAP assays for melon slices were shown in Figs. 1, 2, 3, and 4

TPC of dried melon slices before digestion changed between 233.51 to 719.07 mg GAE/100 g dw (Fig. 1). Drying caused a reduction in TPC of melon slices by 5–47%. On the other hand, there were some drying conditions including Run 1, 3, 4, 10 and 14 which lead to an increment in TPC of melon slices by 2–35%. The wide range in the decomposition ratio can be explained by the stability of the phenolics. Although some phenolics could be very

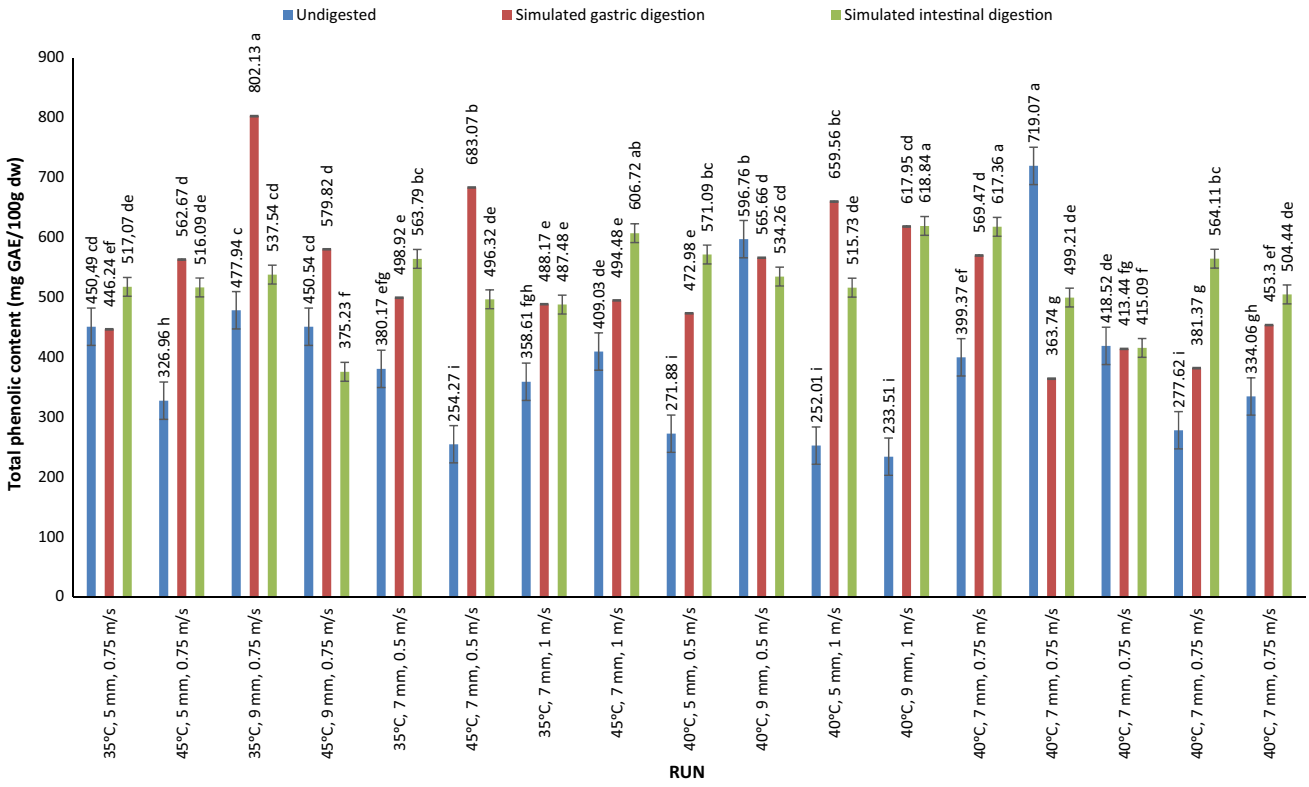

Fig. 1 TPC content of the dried melon samples before digestion, after gastric digestion, and after intestinal digestion. Different small letters indicate statistically significant differences ($p < 0.05$)

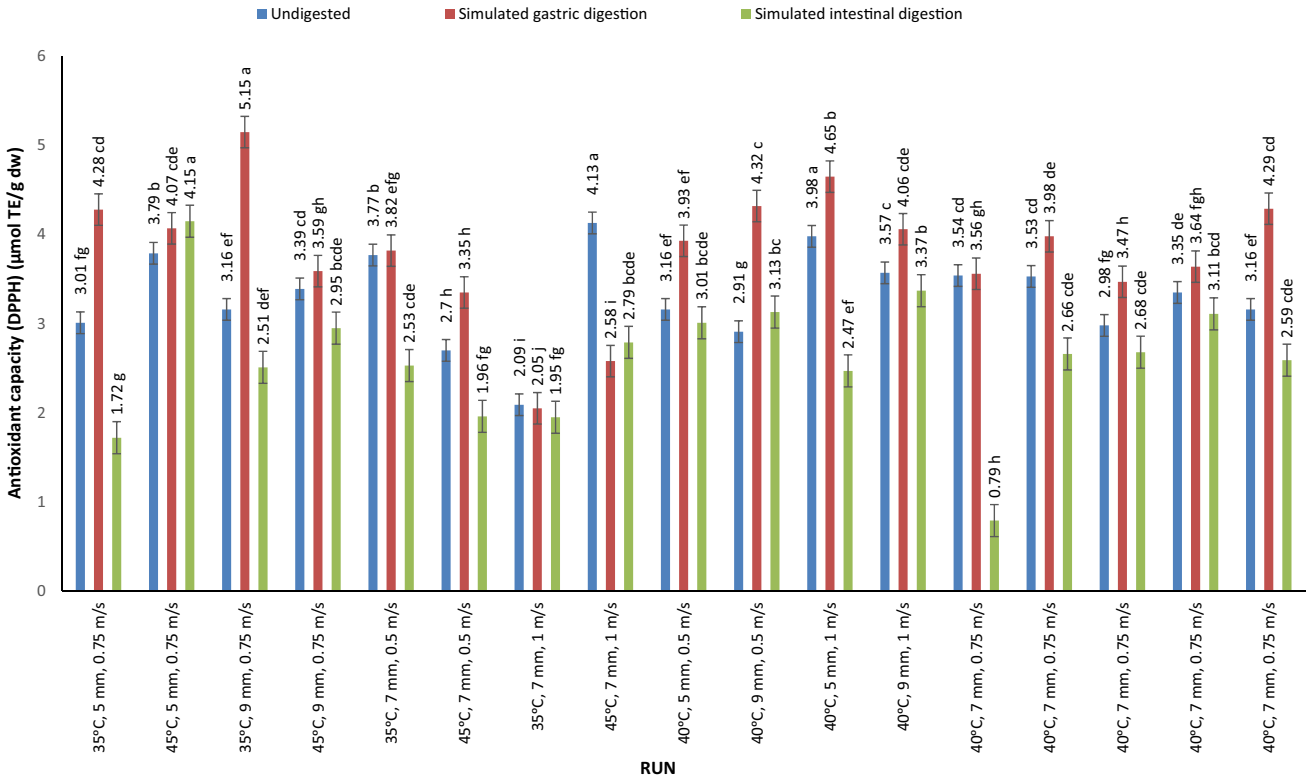

Fig. 2 Antioxidant capacity (DPPH) of the dried melon samples before digestion, after gastric digestion, and after intestinal digestion. Different small letters indicate statistically significant differences ($p < 0.05$)

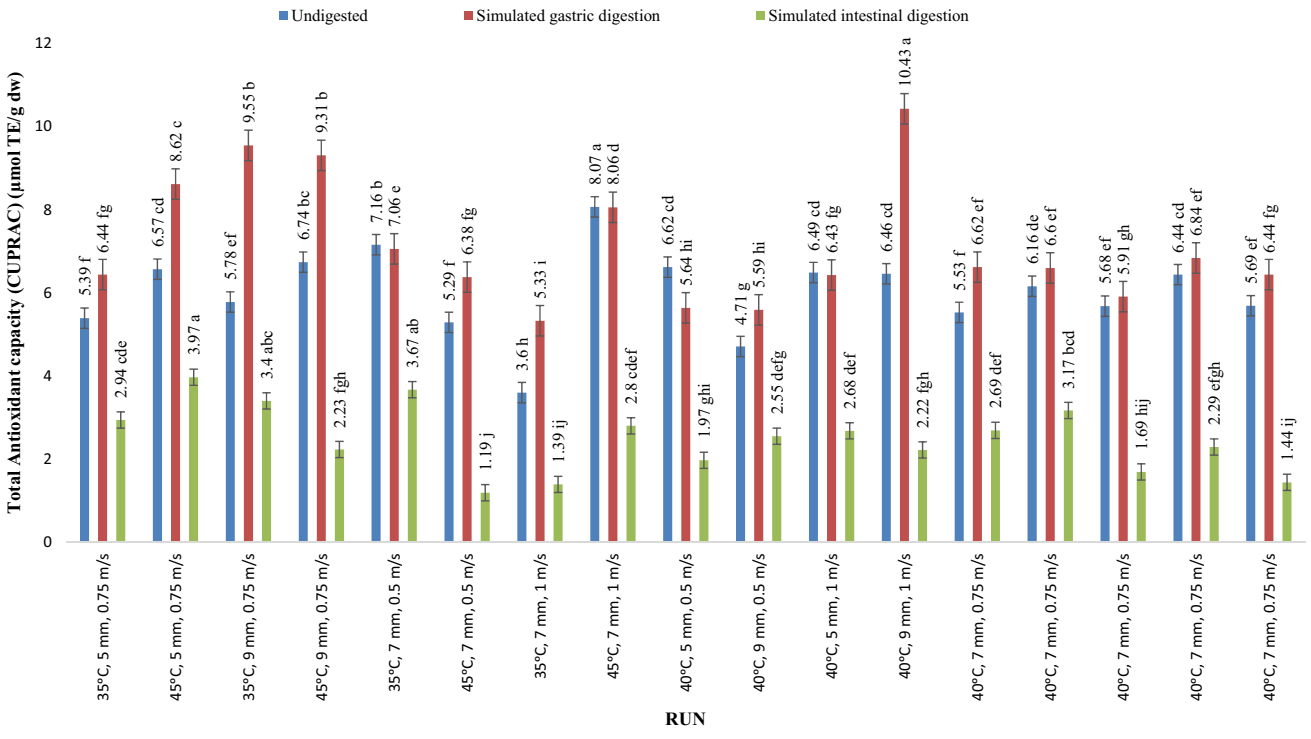

Fig. 3 Antioxidant capacity (CUPRAC) of the dried melon samples before digestion, after gastric digestion, and after intestinal digestion. Different small letters indicate statistically significant differences ($p < 0.05$)

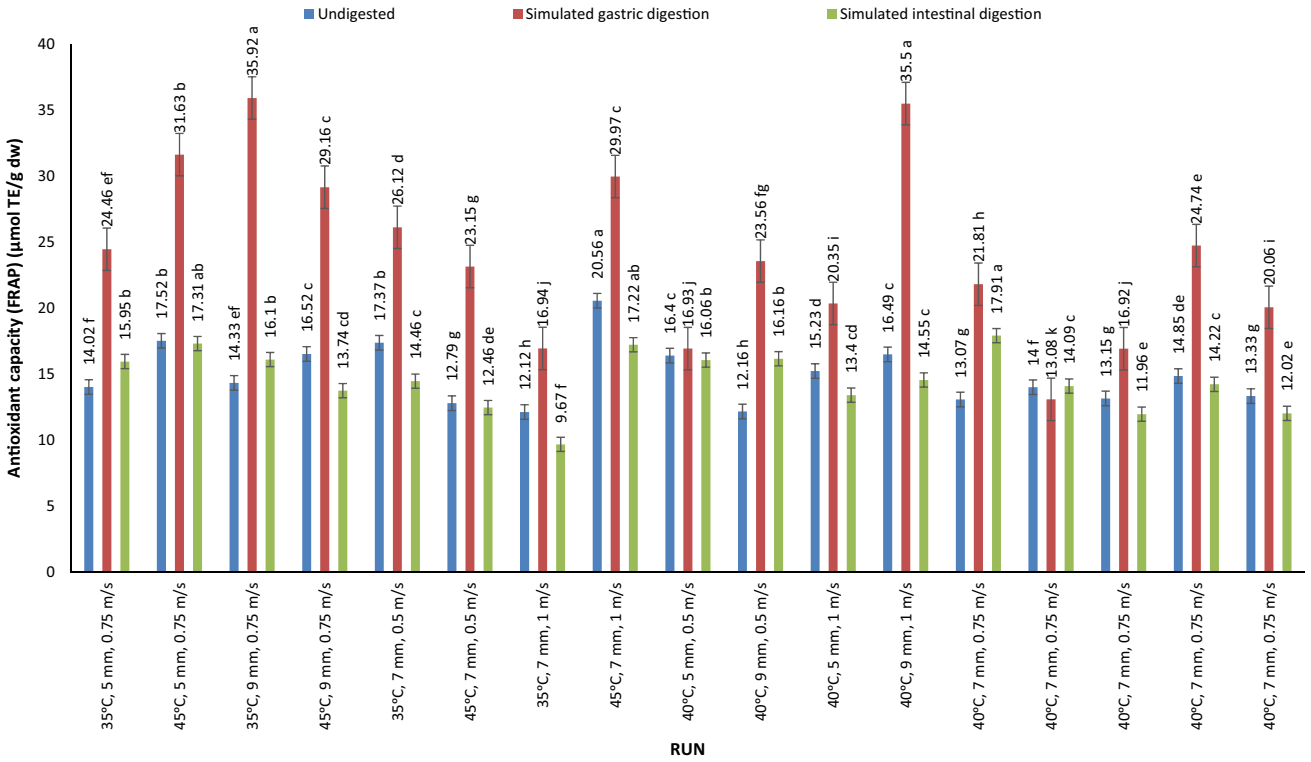

Fig. 4 Antioxidant capacity (FRAP) of the dried melon samples before digestion, after gastric digestion, and after intestinal digestion. Different small letters indicate statistically significant differences ($p < 0.05$)

sensitive to heat treatment, some of them are relatively heat stable [57, 58]. During drying process, phenolics in different foods degrade at unsimilar rates. This can be related to the physical and also physiochemical features of particular phenolic acids which are unique in each product and the interactions of these phenolic acids with other compounds in the food matrix [59]. Moreover, polyphenol oxidase (PPO) in various fruits has different optimum substrates [60, 61]. For that reason, the degradation rate of phenolics caused by PPO activity during drying process changes from product to product [14]. In the same context, compared to our findings, Jin et al. [62] reported higher degredation ratio (appr. 75%) for TPC content in bitter melon subjected to hot air drying and radio frequency assisted hot air drying. The increments in the TPC of the melon slices dried under the aforementioned conditions in our study can be attributed to the release of phenolics bound to the plant cell wall [63]. Consistent with our findings, Ahmed et al. [7] reported that TPC of melons dried in heating systems were higher when comparing to the fresh melon. Moreover, Capanoglu [64] stated that better extractability of compounds from the samples in consequence of break down in cell walls and/or release from sequestration are the possible reasons of the increment of TPC after drying and Nicoli et al. [65] also elucidated this increase as formation of Maillard reaction products having strong AA. In addition, some studies have emerged that dried fruits have a supreme quality of antioxidant features due to the level of polyphenols and also because of the formation of its derivatives in monomer forms attributed to the breakdown or hydrolysis of the complex polymeric molecules during dehydration [66–69].

DPPH values of fresh melon samples was 6.45 µmol TE/g dw (Fig. 2). After drying DPPH values were decreased between 2.09 and 4.13 µmol TE/g dw for undigested samples with a ratio of 35–67%. AA of melon slices measured by CUPRAC assay decreased by 3–30%, on the other hand some of the drying conditions caused an increase in AA (CUPRAC) with 1–30% (Fig. 3). AA of dried samples measured by FRAP assay prevealed an increase changed between 26.38% and 114.39% (Fig. 4). Although heat, light, and oxygen sensitive phytochemicals decompose during drying, thermal treatments can enhance the overall antioxidant potential of processed fruits and vegetables in paticular ways [65, 70]. For this reason, different results have been declared for several fruits and drying conditions [8]. Consistent to our findings, Ahmed et al. [7] reported that drying cause an increment in AA values of melons compared to fresh melon. This can be attributed to the heat intensity, application period and thermal stability of the antioxidant compounds in the fruit. The difference between the mechanisms

of assays [44] may contribute to the different trend in AA of the slices after drying. Moreover, different combination of drying temperature, slices thickness and ait velocity preveailed an unconsistent degradation ratio of AA and TPC of the melon slices in our study. Similarly, Vega-Gálvez et al. [71] investigated the effect of temperature (40, 60, and 80 °C) and drying air velocity (0.5, 1.0, and 1.5 m/s) on quality characteristics of apple slices. The researchers determined that the TPC reduced with increase in temperature, but a reduced thermal degradation was determined at high air velocity. On the contrary, there was the least destruction of phenolics at 80 °C and 1.5 m/s, likely due to short drying period and, therefore, less exposure of the phenolics to thermal effect. The rise in temperature in drying may cause decrement of phenolic compounds, however, depending on the drying air velocity and on the heat exposure duration, the antioxidant compounds content, as well as the AA, could be affected [71–73].

Generally, TPC results of dried melon samples of simulated gastric and intestinal digestion were higher than undigested dried melons (Fig. 1). This increment reached 168.64% (Run 6) in the stomach phase and 165.02% (Run 12) in the intestinal phase when compared with undigested TPC results. In coherent with our results, Kamiloglu et al. [74] also stated an increase in TPC after intestinal digestion of cakes enriched with black carrot pomace. These increments in TPC after simulated intestinal digestion could be related to the augmented high release of phenolics from the matrix in consequence of heat treatment [27].

Comparing to gastric (2.01 µmol TE/g dw) and intestinal (1.44 µmol TE/g dw) digested fresh samples, DPPH values of the gastric and intestinal digested dried melons were increased (Fig. 2). This increament reached 156.22% (Run 3) in the stomach phase and 188.19% (Run 2) in the intestinal phase when compared with undigested DPPH results of fresh melons. Samples (slice thickness of 7 mm) dried at 35 °C with 1 m/s drying air velocity (Run 7) had the lowest DPPH values for both undigested and gastric digested extracts. However, when drying temperature reached to 45 °C (Run 8), DPPH values of undigested was also the highest. The loss of AA (DPPH) of intestinal digested extract of dried melons was reached to 77.68%. As can be seen from Fig. 3, CUPRAC values of all intestinal digested samples of dried melon samples were significantly reduced when compared undigested and gastric digested samples. It can be monitored that AA (CUPRAC) loss of intestinal digested extracts of the dried samples was changeable as degradation of this component ranged from 39.57 to 77.50% depending on the operating conditions. As could be seen from Fig. 4, FRAP values of all gastric digested extracts of dried melon samples were significantly increased. On the other hand, after gastric digestion, a decrease with a ratio of 2.07–20.21% was observed in the intestinal phase.

Fitting the models

Table 2 showed the Box–Behnken design matrix including uncoded independedent variables. Design Expert 9 software was used to generate polynomial equations, and Table 4 summarized regression analysis including regression coefficient, lack of fit, R^2, adjusted R^2, p values and consequently proper models. The coeficients for the equations were considered significant if F-value was less than 0.05 showed the significance of the model terms. Lack of fit values were considered non-signifance in case p value > 0.05, which indicated that polynomial model fits the design. Moreover, The R^2 and Adj R^2 value greater than 0.80 indicated that the model was statistically significant [75].

Based on those criteria, reduced quadratic model was found as the best model for TPC (Undigested, Simulated gastric digested, Simulated intestinal digested) and AA measured by CUPRAC (Simulated intestinal digested) and FRAP (Undigested, Simulated gastric digested, Simulated intestinal digested), whereas reduced cubic model was fitted for AA from DPPH (Simulated gastric digested, Simulated intestinal digested) and CUPRAC (Undigested, Simulated gastric digested) ($p < 0.05$) assays. DPPH (Undigested) can be estimated using the quadratic model ($p < 0.05$). Lack of fit values were determined to be insignificant for all models ($p > 0.05$) and the developed models could adequately predict the responses (Table 4). High R^2 and adjusted R^2 values indicated a good agreement between experimental and predicted values. The highest R^2 (0.9865) and adjusted R^2 (0.9639) values were found in Y8 (CUPRAC-Simulated gastric digestion), while the lowest values were observed in Y2 (TPC-Simulated gastric digestion) as 0.7604 and 0.5507, respectively.

Post in vitro digestion of total phenolic content

TPC-undigested (Y1)

TPC (undigested) (Y1) of the dried melon slices changed between 233.51 ± 6.86 and 719.07 ± 61.77 mg GAE/100 g dw. The reduced quadratic model for TPC (undigested) value can be expressed by the following Eq. (2):

$$\begin{aligned} Y1\,(TPC-Undigested) &= 374.620 - 28.300X_1 + 11.690X_2 + 14.250X_3 \\ &+ 24.030X_1X_2 + 44.080X_1X_3 - 176.830X_2X_3 \\ &- 17.080X_1^2 + 61.920X_2^2 \end{aligned} \quad (2)$$

According to Eq. 2, while drying air temperature (X_1) had negative correlation, slice thickness (X_2) and drying air velocity (X_3) had positive correlation on TPC (undigested). Moreover, it was negatively influenced by the quadratic term

Table 4 Summary of regression analysis response

Regression coefficient	Y1	Y2	Y3	Y4	Y5	Y6	Y7	Y8	Y9	Y10	Y11	Y12
b_0	374.620	434.800	472.910	3.312	3.790	2.530	6.020	6.482	1.890	13.680	19.640	13.070
X_1 Drying air temperature	−28.300	10.570	8.700	0.248		0.068	0.593*	0.499*	−0.151	1.190*	−0.200	1.270*
X_2 Slice thickness	11.690	99.610*	15.870	−0.114				0.969*	−0.145	−0.459	3.850*	0.430
X_3 Drying air velocity	14.250	−41.650		0.154				1.410*	−0.036	0.710*	3.130	−0.538
$X_1 X_2$	24.030	84.690		−0.138	−0.3375	−0.498*		−0.605*	−0.550	−0.328	−3.480	−2.330*
$X_1 X_3$	44.080		46.680*	0.777*		0.353	1.580*	0.853*	0.976*	3.260*	0.982	2.390*
$X_2 X_3$	−176.830*	59.620	34.990	−0.040			0.470*	1.012*		1.370*	2.130	
X_1^2	−17.080	108.200*	18.720	−0.103	−0.4028*			0.842*	0.508	1.280*	7.010*	−0.145
X_2^2	61.920	52.890	40.120	0.129	0.8873*	0.380*		1.160*	0.600*	0.639	4.040	1.450
X_3^2			46.940*	−0.036	−0.4352*			−0.616*		0.751		0.525
$X_1^2 X_3$					−0.6350*			−1.420*				
$X_1 X_2^2$					−0.4425*	0.650*						
$X_2^2 X_3$							0.405*					
$X_2 X_3^2$							−0.485*					
Lack of Fit	0.3936	0.6123	0.9832	0.2248	0.5915	0.2491	0.8751	0.9826	0.6828	0.6146	0.7275	0.6652
R^2	0.8880	0.7604	0.8344	0.8437	0.8753	0.7868	0.9399	0.9865	0.7944	0.9594	0.8327	0.8838
Adj R^2	0.7087	0.5507	0.6413	0.6426	0.8004	0.6802	0.9126	0.9639	0.6145	0.9071	0.6416	0.7290
p value	0.0473	0.0456	0.0472	0.0359	0.0005	0.0039	0.0001	0.0001	0.0268	0.0005	0.0339	0.0239
Model	Reduced quadratic	Reduced quadratic	Reduced quadratic	Quadratic	Reduced cubic	Reduced cubic	Reduced cubic	Reduced cubic	Reduced quadratic	Reduced quadratic	Reduced quadratic	Reduced quadratic

*Significant at $p < 0.05$

of drying air temperature (X_1^2) ($p < 0.05$). Maximum TPC (undigested) was determined at Run 14. However, minimum TPC (undigested) was obtained at Run 12. The interaction term of slice thickness (X_2) and drying air velocity (X_3) had significant effect on the TPC-Undidested values of dried samples ($p < 0.05$). 3D surface plots for TPC-Undigested demonstrates that higher drying temperature and low slice thickness led to decrement in TPC-Undigested (Fig. 5a). Figure 5b demonstrates that increase of drying air temperature and decrease in drying air velocity resulted in lower amount of TPC – Undigested. Figure 5c reveals that negative correlation between slice thickness and drying air velocity. TPC increased as a result of the decrease in air velocity with the increase in slice thickness and the increase in air velocity with the decrease in slice thickness (Fig. 5c).

TPC-simulated gastric digested (Y2)

TPC (simulated gastric digested) (Y2) changed between 381.37 ± 43.51 and 802.13 ± 29.11 mg GAE/100 g dw. The reduced quadratic model for TPC (simulated gastric digested) value can be expressed by the following Eq. (3):

$$Y2\ (TPC - Simulated\ gastric\ digested) = 434.800 + 10.570X_1 + 99.610X_2 - 41.650X_3 + 84.690X_1X_2 + 59.620X_2X_3 + 108.200X_1^2 + 52.890X_2^2 \quad (3)$$

According to Eq. 3, drying air temperature (X_1) and slice thickness (X_2) had positive correlation, whereas drying air velocity (X_3) had negative correlation with TPC (simulated gastric digested). While maximum TPC (simulated gastric digested) was determined at Run 3, minimum TPC (undigested) was obtained for the slices dried with Run 16 conditions. The linear term of slice thickness (X_1) and the quadratic term of drying air temperature (X_1^2) significantly affected TPC—Simulated gastric digested ($p < 0.05$). The graphical representation of the influence of slice thickness and air temperature on TPC—Simulated gastric digested (Fig. 5d) reveals that when air temperature decrased to 40 °C

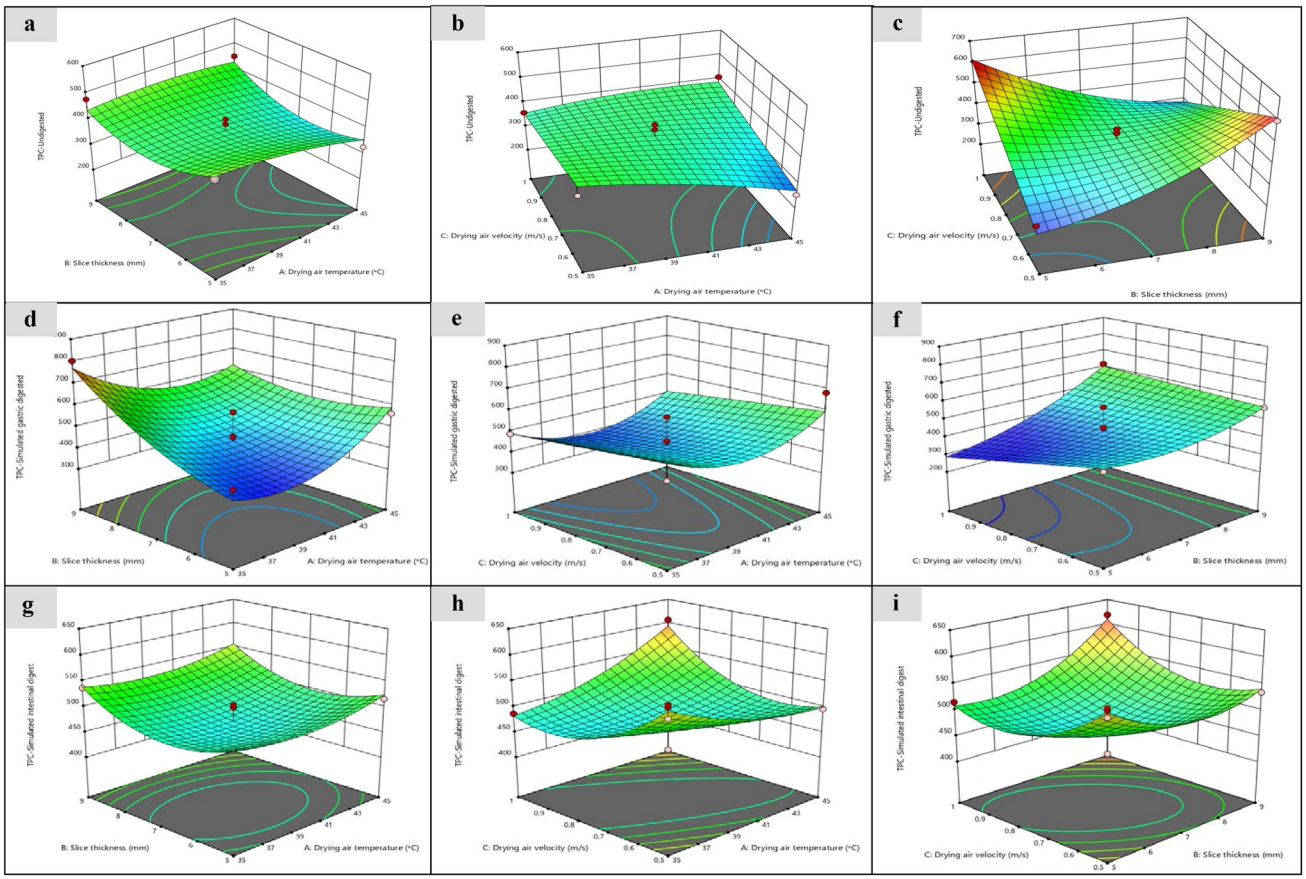

Fig. 5 3D surface graphs showing the effects of drying air temperature, slice thickness and drying air velocities on TPC-undigested, TPC-simulated gastric digested and TPC-simulated intestinal digested (mg GAE/100 g dw)

and slice thickness below 7 mm was applied, TPC—Simulated gastric digested was the lowest. In Fig. 5e, it can be observed that when drying air temperature was between 37 and 41 °C and drying air velocity was 0.8–1 m/s the lowest TPC—Simulated gastric digested was obtained. Figure 5f demonstrates that increase of slice thickness resulted in higher amount of TPC—Simulated gastric digested.

TPC-simulated intestinal digested (Y3)

TPC (simulated intestinal digested) (Y3) changed between 375.23 ± 24.23 and 618.84 ± 16.69 mg GAE/100 g dw. The quadratic model for TPC (simulated intestinal digested) can be expressed by the following Eq. (4).

$$Y3\ (TPC - Simulated\ intestinal\ digested) = 472.910 + 8.700X_1 + 15.870X_2 + 46.680X_1X_3 + 34.960X_2X_3 + 18.720X_1^2 + 40.120X_2^2 + 46.940X_3^2 \quad (4)$$

While air temperature (X_1) and slice thickness (X_2) had positive correlation, air velocity (X_3) had no correlation with TPC (simulated intestinal digested). Moreover, it was significantly positive influenced by the interaction term of drying air temperature- slice thickness (X_1X_2) and the quadratic term drying air velocity (X_3^2) ($p < 0.05$). Maximum TPC (simulated intestinal digested) was determined in Run 12. However, minimum TPC (simulated intestinal digested) was found in Run 4. 3D surface plots for TPC-Simulated intestinal digested demonstrates that when both drying air temperature (> 40 °C) and slice thickness increased (> 8 mm) TPC-Simulated intestinal digested was significantly higher (5 g). Moreover, Fig. 5g shows that the lowest drying air temperature and slice thickness caused the increment in TPC-Simulated intestinal digested. From Fig. 5h it can be observed that highest drying air velocity (< 0.9 m/s) and increased air temperature (> 43 °C) lead to higher TPC-Simulated intestinal digested. Figure 5i shows that an increment in air velocity and slice thickness resulted in higher TPC-Simulated intestinal digested. In the opposite manner, the decrease in air velocity and slice thickness lead to higher TPC-Simulated intestinal digested.

Post in vitro digestion of antioxidant activity

DPPH-undigested (Y4)

AA (DPPH-Undigested) (Y4) changed between 2.09 ± 0.07 and 4.13 ± 0.16 (µmol TE/g dw). The quadratic model for AA (DPPH-Undigested) value can be expressed by the following Eq. (5):

According to Eq. (5), while air temperature (X_1) and air velocity (X_3) had positive correlation, slice thickness (X_2) had negative correlation with AA (DPPH-Undigested). Moreover, it was positively influenced by the quadratic terms of slice thickness (X_2^2). Quadratic terms of air temperature (X_1^2) and air velocity (X_3^2) had negative effect on the former. Moreover, it was significantly positively influenced by the interaction term of drying air temperature-drying air velocity (X_1X_3) ($p < 0.05$). Maximum AA (DPPH-Undigested) was determined in Run 8. However, minimum AA (DPPH-Undigested) was found in Run 7. 3D surface plots for AA (DPPH-Undigested) shows that increase in air temperature (> 37.5 °C) and decrease in slice thickness (< 7 mm) caused an increase in AA measured by DPPH assay in undigested samples (Fig. 6a). From Fig. 6b, it can be monitored that increased air velocity (> 0.8 m/s) and air temperature (> 40 °C) had positive influence on AA (DPPH-Undigested). It can be seen that lower slice thickness and higher air velocity resulted in increased AA (DPPH-Undigested) (Fig. 6c).

DPPH- Simulated gastric digested (Y5)

AA (DPPH- Simulated gastric digested) (Y5) changed between 2.05 ± 0.22 and 5.15 ± 0.08 µmol TE/g dw. The reduced cubic model for AA (DPPH-simulated gastric digested) value can be expressed by the following Eq. (6):

$$Y5\ (DPPH - Simulated\ gastric\ digested) = 3.790 - 0338X_1X_2 - 0.403X_1^2 + 0.8887X_1^2 - 0.403X_1^2 + 0.887X_2^2 - 0.435X_3^2 - 0.635X_1^2X_3 - 0.443X_1X_2^2 \quad (6)$$

According to Eq. (6), the interaction term of drying air temperature- slice thickness (X_1X_2) had negative effect on AA (DPPH-Simulated gastric digested) whereas the square of slice thickness (X_2^2) was significantly positive correlation ($p < 0.05$) on it. The quadratic terms of drying air temperature (X_1^2), drying air velocity (X_3^2) and interaction–quadratic terms of drying air temperature and drying air velocity ($X_1^2X_3$), drying air temperature and slice thickness ($X_1X_2^2$) showed also negative effects on AA (DPPH-simulated gastric digested) value ($p < 0.05$). Maximum AA (DPPH- Simulated gastric digested) was determined for in Run 3. Similar

$$Y4\ (DPPH - Undigested) = 3.312 + 0.248X_1 + 0.114X_2 + 0.154X_3 - 0.138X_1X_2 + 0.777X_1X_3 - 0.040X_2X_3 - 0.103X_1^2 + 0.129X_2^2 - 0.036X_3^2 \quad (5)$$

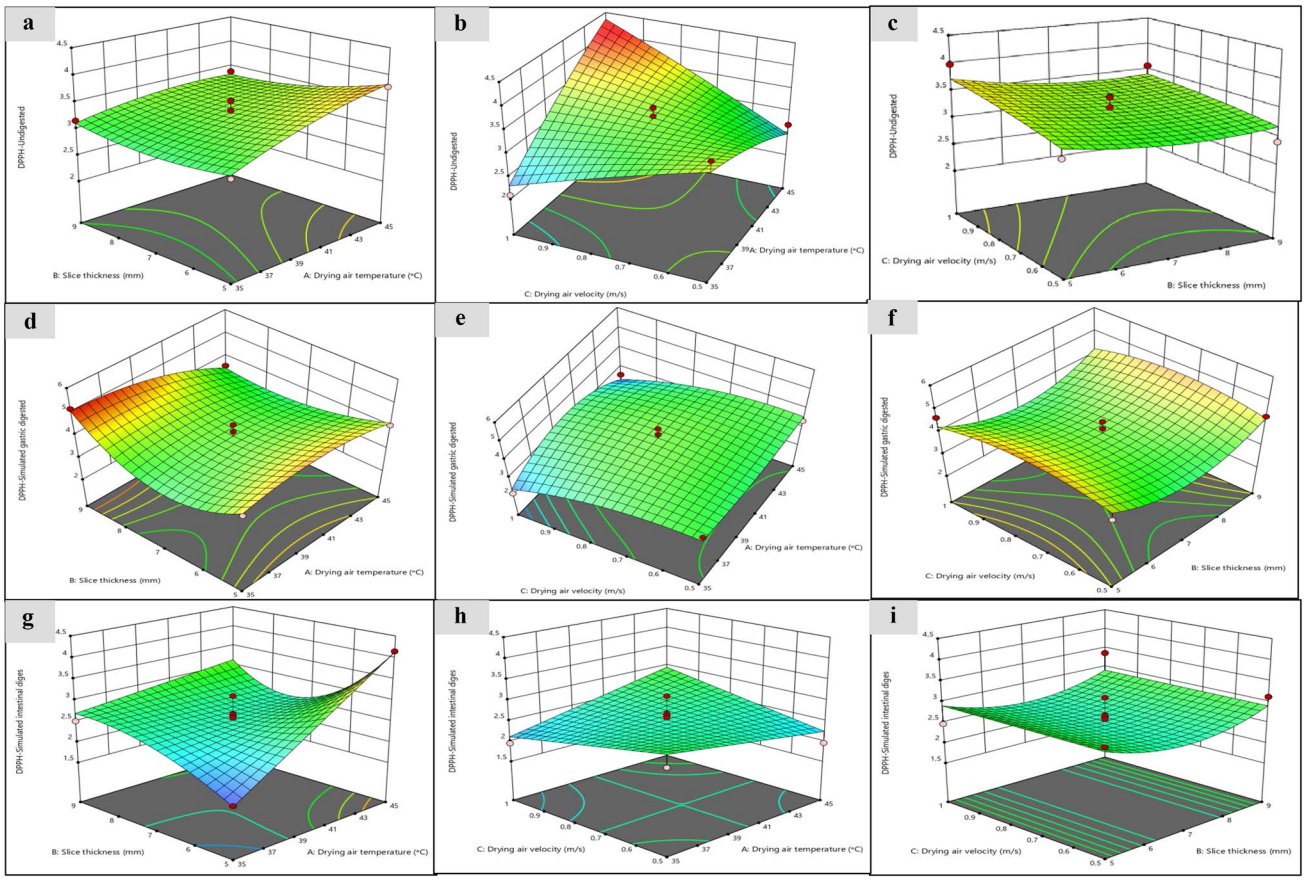

Fig. 6 3D surface graphs showing the effects of drying air temperature, slice thickness and drying air velocities on DPPH-undigested, DPPH-simulated gastric digested and DPPH-simulated intestinal digested (μmol TE/g dw)

to AA (DPPH-Undigested), minimum AA (DPPH-simulated gastric digested) was also found in Run 7. The graphical representation of the influence of slice thickness and air temperature on AA (DPPH- Simulated gastric digested) (Fig. 6d) reveals that the DPPH- Simulated gastric digested values of dried samples increased with decreasing drying air temperature and increasing slice thickness. Figure 6e shows that when slice when slice thickness was between 5 and 9 mm and air velocity was 0.6–0.9 m/s, the highest DPPH- Simulated gastric digested value was obtained. Drying processes with drying air temperature ranging between 35 and 45 °C and drying air velocity higher than 0.9 m/s lead to dried melon slices having the lowest AA (DPPH) after the simulated gastric digestion (Fig. 6f).

DPPH-simulated intestinal digested (Y6)

AA (DPPH- simulated intestinal digested) (Y6) changed between 0.79 ± 0.19 and 4.15 ± 0.21 μmol TE/g dw. The reduced cubic model for AA (DPPH- simulated intestinal digested) value can be expressed by the following Eq. (7):

$$Y6\ (DPPH - \text{Simulated intestinal digested}) = 2.530 + 0.068X_1 - 0.498X_1X_2 + 0.353X_1X_3 0.380X_2^2 + 0.052X_3 + 0.650X_1X_2^2 \quad (7)$$

From Eq. (7), it can be observed that linear term of X_1 and the interaction term of drying air temperature- drying air velocity (X_1X_3) had positive impact on AA (DPPH- Simulated intestinal digested), but the interaction term of drying air temperature- slice thickness (X_1X_2) had significantly negative ($p < 0.05$) impact on the former. Moreover, the quadratic term of slice thickness (X_2^2) and interaction–quadratic terms of drying air temperature and slice thickness ($X_1 X_2^2$) significantly positive effect on DPPH- Simulated intestinal digested ($p < 0.05$). The highest and lowest AA (DPPH-Simulated intestinal digested) values were obtained with the drying processes specified as Run 2 and Run 13,

respectively. 3D surface plots shows that DPPH-Simulated intestinal digested decreased when both air temperature and slice thickness decreased. Moreover when slice thickness and drying air temperature came close to respectively 5 mm and 45 °C, DPPH-Simulated intestinal digested increased (Fig. 6g). It can be observed that higher air temperature and air velocity had positive influence on DPPH-Simulated intestinal digested (Fig. 6h). In the DPPH (Simulated intestinal digested) results, a parabolic decrease was observed with increasing slice thickness and a parabolic increase was shown with increasing slice thickness after the midpoint (7 mm) (Fig. 6i).

CUPRAC-undigested (Y7)

AA (*CUPRAC-Undigested*) (Y7) changed between 3.60 ± 0.06 and 7.16 ± 0.17 µmol TE/g dw. The reduced cubic model for AA (*CUPRAC-Undigested*) value can be expressed by the following Eq. (8):

According to Eq. (8), air temperature (X_1), the interaction term of drying air temperature—drying air velocity (X_1X_3), slice thickness—drying air velocity (X_2X_3) and interaction–quadratic terms of slice thickness—drying air velocity ($X_2^2X_3$) had significantly positive correlation on AA (CUPRAC-Undigested), whereas it was negative influenced by interaction–quadratic terms of slice thickness—drying air velocity ($X_2X_3^2$). Maximum AA (DPPH-Simulated gastric digested) was determined in Run 5. Similarly to AA (DPPH-Undigested), minimum AA (CUPRAC-Undigested) was also found in Run 7. 3D surface plots depicts that the CUPRAC values of the samples showed a linear decrease with decreasing drying air temperature (Fig. 7a). It can be observed that the highest CUPRAC-Undigested was obtained when maximum air temperature (45 °C) applied and drying air velocity (1 m/s) (Fig. 7b). Figure 7c demonstrates that > 7 mm slice thickness and air velocity < 0.7 m/s resulted in lower CUPRAC-Undigested value.

$$Y7\ (CUPRAC-Undigested) = 6.020 + 0.593X_1 + 1.580X_1X_3 + 0.470X_2X_3 + 0.405X_2^2X_3 - 0.485X_2X_3^2 \quad (8)$$

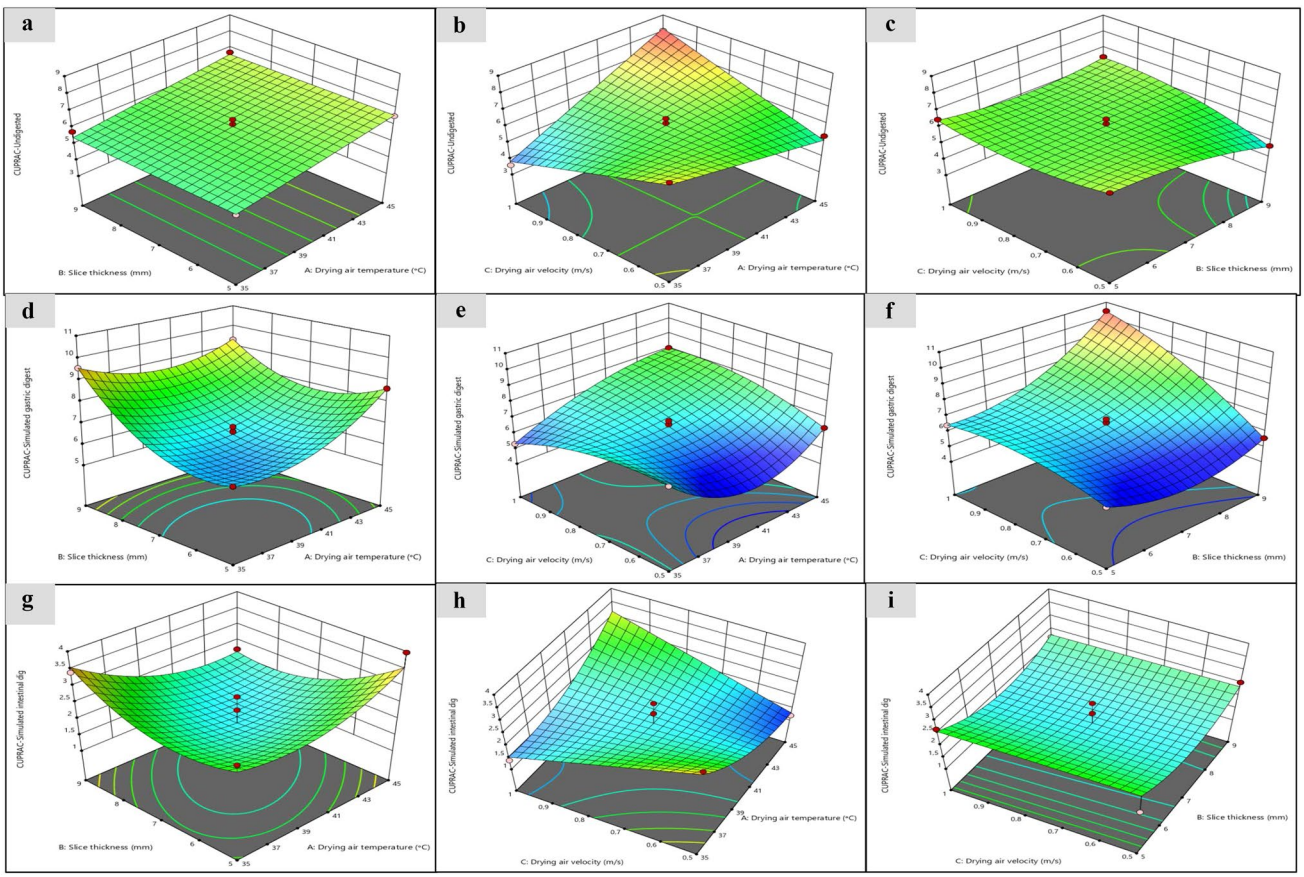

Fig. 7 3D surface graphs showing the effects of drying air temperature, slice thickness and drying air velocities on CUPRAC-undigested, CUPRAC-simulated gastric digested and CUPRAC-simulated intestinal digested (µmol TE/g dw)

CUPRAC-simulated gastric digested (Y8)

AA (CUPRAC- Simulated gastric digested) (Y8) changed between 5.33 ± 0.06 and 10.43 ± 0.12 µmol TE/g dw. The reduced cubic model for AA (CUPRAC-Simulated gastric digested) can be expressed by the following Eq. (9).

$$\begin{aligned} Y8\,(CUPRAC-Simulated\ gastric\ digested) &= 6.482 + 0.499\,X_1 + 0.969\,X_2 + 1.410X_3 \\ &- 0.605\,X_1X_2 + 0.853\,X_1X_3 + 1.012\,X_2X_3 \\ &+ 0.842\,X_1^2 + 1.160\,X_2^2 - 0.616\,X_3^2 - 1.420\,X_1^2X_3 \end{aligned} \quad (9)$$

From Eq. (9), it can be observed that all linear terms of X_1, X_2, X_3 (air temperature, slice thickness, air velocity) and the interaction terms of drying air temperature—drying air velocity (X_1X_3), slice thickness—drying air velocity (X_2X_3) had positive impact ($p < 0.05$) on AA (CUPRAC- simulated gastric digested). Moreover, it was negatively influenced by the interaction term of drying airtemperature—slice thickness (X_1X_2), the quadratic terms of air velocity (X_3^2) and interaction–quadratic terms of drying air temperature and drying air velocity ($X_1^2X_3$) ($p < 0.05$). Quadratic term of air temperature and slice thickness (X_1^2 and X_2^2) had positive effect on the former ($p < 0.05$). The highest AA (CUPRAC—Simulated gastric digested) value (10.43 ± 0.12 mg GAE/100 g dw) was found at Run 12. The lowest AA (CUPRAC- simulated gastric digested) (5.33 ± 0.06 mg GAE/100 g dw) was found at Run 7, as well as AA (DPPH-Simulated gastric digested). The graphical representation of the influence of slice thickness and air temperature on CUPRAC-Simulated gastric digested value (Fig. 7d) shows that when air temperature ranged between 38 and 43 °C and the highest slice thickness (9 mm) was applied, CUPRAC-simulated gastric digested value was the highest. Minimum CUPRAC-Simulated gastric digested value was obtained when air temperature ranged between 35 and 41 °C applied to melon slices having thickness below 7 mm. From Fig. 7e it can be observed that when the drying air velocity below 0.6 m/s and drying air temperature between 37.5 and 43 °C, the lowest CUPRAC-Simulated gastric digested value was obtained. Morever, air temperature at 45 °C with air velocity > 0.9 m/s caused the highest CUPRAC-Simulated gastric digested value. Figure 7f shows that air velocity higher than 0.8 m/s and 9 mm slice thickness resulted in highest CUPRAC-Simulated gastric digested value.

CUPRAC-simulated intestinal digested (Y9)

AA (CUPRAC- Simulated intestinal digested) (Y9) changed between 1.19 ± 0.12 and 3.97 ± 0.90 µmol TE/g dw. The reduced quadratic model for AA (CUPRAC-Simulated intestinal digested) can be expressed by the following Eq. (10).

$$\begin{aligned} Y9\,(CUPRAC-Simulated\ intestinal\ digested) &= 1.890 - 0.151\,X_1 - 0.145\,X_2 - 0.036\,X_3 - 0.550\,X_1X_2 \\ &+ 0.976\,X_1X_3 + 0.508X_1^2 + 0.600X_2^2 \end{aligned} \quad (10)$$

According to Eq. (10), model terms for CUPRAC (Simulated intestinal digested) value of dried samples samples were negative on all linear terms of drying air temperature, slice thickness, air velocity (X_1, X_2, X_3) and the interaction term of drying air temperature—slice thickness (X_1X_2). However the interaction term of drying air temperature—air velocity (X_1X_3) and quadratic terms of drying air temperature (X_1^2) and slice thickness (X_2^2) had positive correlation on AA (CUPRAC-Simulated intestinal digested). Among these terms the interaction term of drying air temperature—air velocity (X_1X_3) and quadratic term of slice thickness (X_2^2) showed significant effect on CUPRAC-Simulated intestinal digested ($p < 0.05$). Similarly to AA (DPPH-simulated intestinal digested), maximum AA (CUPRAC-Simulated intestinal digested) was determined in Run 2. Minimum AA (CUPRAC- Simulated intestinal digested) was found in Run 6. 3D surface plots depicts that CUPRAC-Simulated intestinal digested value was minimum when air temperature was higher than 37.5 °C and slice thickness was higher than 6 mm. Besides that, when air temperature was between 41 and 45 °C and slice thickness was below 6 mm, CUPRAC-Simulated intestinal digested value was the highest (Fig. 7g). It can be observed that air velocity below than 0.55 m/s and air temperature higher 42.5 °C resulted in the lowest CUPRAC-Simulated intestinal digested value (Fig. 7h). Moreover, air temperature lower 36 °C with air velocity below than 0.7 m/s gave the highest result. In the CUPRAC (Simulated intestinal digested) results, a parabolic decrease was observed with increasing slice thickness and after the midpoint (7 mm) of slice thickness a parabolic increase was shown (Fig. 7i).

FRAP-undigested (Y10)

AA (FRAP- Undigested) (Y10) of the dried melon slcies changed between 12.12 ± 0.16 and 20.56 ± 0.17 µmol TE/g dw. The reduced quadratic model for AA (*FRAP-Undigested*) can be expressed by the following Eq. (11).

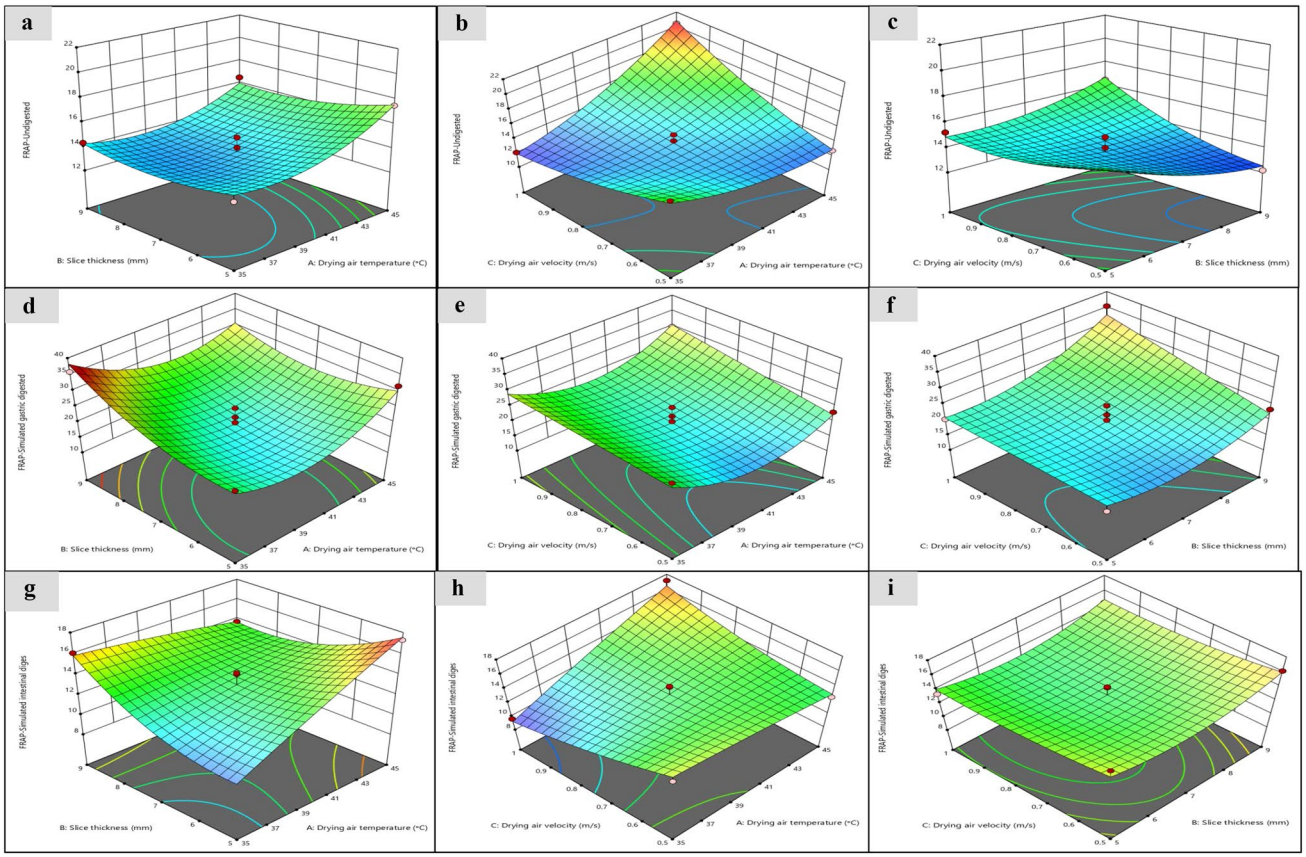

Fig. 8 3D surface graphs showing the effects of drying air temperature, slice thickness and drying air velocities on FRAP-undigested, FRAP-simulated gastric digested and FRAP-simulated intestinal digested (μmol TE/g dw)

$$Y10\,(FRAP-Undigested) = 13.680 + 1.190\,X_1 - 0.459\,X_2 + 0.710\,X_3 - 0.328\,X_1X_2 + 3.260\,X_1X_3 + 1.370\,X_2X_3 + 1.280\,X_1^2 + 0.639\,X_2^2 + 0.751\,X_3^2 \quad (11)$$

From Eq. (11), it can be monitored that both linear terms of X_1 and X_3 (air temperature and air velocity) had significantly positive impact ($p<0.05$) on AA (FRAP-Undigested), but the linear term of slice thickness (X_2) and the interaction term of drying air temperature—slice thickness (X_1X_2) had negative impacts on the former. Moreover, AA (FRAP-Undigested), was positively influenced by the quadratic terms of all parameters (X_1^2, X_2^2 and X_3^2). The interaction terms of drying air temperature—air velocity (X_1X_3) and slice thickness—air velocity (X_2X_3) for FRAP (Undigested) value of dried samples were significantly negative ($p<0.05$). While the highest AA (FRAP-Undigested) was found at Run 8, the lowest AA (FRAP-Undigested) was found at Run 7. Similarly, (DPPH-Undigested) minimum and maximum AA (FRAP-Undigested) values were determined at Run 7 and Run 8, respectively. The FRAP (Undigested) values of the dried samples indicated a parabolic decrease with decreasing drying air temperature (Fig. 8a). Moreover when drying air temperature and slice thickness were higher than 42.5 °C and 7.5 mm, respectively, FRAP-Undigested value gained its highest level. Above 0.85 m/s of air velocity and 42.5 °C of air temperature, higher FRAP Undigested value was observed (Fig. 8b). Figure 8c demonstrates that air velocity below 0.6 m/s and slice thickness between 8 and 9 mm resulted in the lowest FRAP-Undigested value.

FRAP-simulated gastric digested (Y11)

AA (FRAP- Simulated gastric digested) (Y11) changed between 13.08 ± 0.47 and 35.92 ± 0.74 μmol TE/g dw. The reduced quadratic model for AA (FRAP-Simulated gastric digested) can be expressed by the following Eq. (12).

$$Y11\,(FRAP-Simulated\ gastric\ digested) = 19.640 - 0.200\,X_1 + 3.85\,X_2 + 3.130\,X_3 - 3.480\,X_1X_2 + 0.982\,X_1X_3 + 2.130\,X_2X_3 + 7.010\,X_1^2 + 4.040\,X_2^2 \quad (12)$$

According to Eq. (12), the linear terms of slice thickness (X_2) and air velocity (X_3); the interaction terms of drying air

temperature—air velocity (X_1X_3) and slice thickness—air velocity (X_2X_3); and also both quadratic terms of air temperature and slice thickness had positive correlation with AA (FRAP- Simulated gastric digested). However the linear term of drying air temperature (X_1) and the interaction term of drying air temperature—slice thickness (X_1X_2) had a negative correlation with the former. Among these terms the linear term of slice thickness and quadratic term of drying air velocity (X_1^2) showed significant effect on FRAP-Undigested values ($p < 0.05$). Similar to AA (DPPH-Simulated gastric digested), maximum AA (FRAP- Simulated gastric digested) was determined in Run 3. Minimum AA (FRAP-Simulated gastric digested) was found in Run 14. 3D surface plots depicted that FRAP-Simulated gastric digested value was minimum when air temperature was between 36 and 41 °C and slice thickness was below 7 mm. (Fig. 8d). It can be observed that air velocity below 0.6 m/s and air temperature between 39 and 44 °C resulted in lowest FRAP-Simulated gastric digested value (Fig. 8e). Figure 8f demonstrated that slice thickness between 5 and 8 mm and air velocity below 0.7 m/s resulted in lowest FRAP-Simulated gastric digested value.

FRAB-simulated intestinal digested (Y12)

AA (FRAP-Simulated intestinal digested) (Y12) changed between 9.67 ± 0.85 and 17.91 ± 0.96 µmol TE/g dw. The reduced quadratic model for AA (FRAP- Simulated intestinal digested) can be expressed by the following Eq. (13).

From Eq. (13), it can be monitored that while both linear terms of air temperature (X_1) and slice thickness (X_2) had positive impact on AA (FRAP- Simulated intestinal digested), the other linear term of air velocity (X_3) had negative impact on it. AA (FRAP- Simulated intestinal digested) was negatively influenced by the interaction term of drying air temperature—slice thickness (X_1X_2) and the quadratic terms of drying air temperature (X_1^2), whereas the interaction term of drying air temperature—air velocity (X_1X_3) and the quadratic terms of slice thickness (X_2^2) and drying air velocity (X_3^2) had positive effect on the former. Among these terms the linear term of slice thickness and the interaction terms of drying air temperature—slice thickness (X_1X_2), drying air temperature—air velocity (X_1X_3) showed significant effect on FRAP-Undigested values ($p < 0.05$). The highest AA (FRAP- Simulated intestinal digested) value was found at Run 13. The lowest AA (FRAP- Simulated intestinal digested) was found at Run 7. Simulated intestinal digested value (Fig. 8g) shows that when air temperature was higher than 40 °C and the applied slice thickness ranged between 5.0 and 5.5 mm. Figure 8h shows that when air temperature and air velocity were respectively higher than 43 °C and 0.8 m/s the highest FRAP-Simulated intestinal digested value was obtained. Figure 8i demonstrates that air velocity above 0.9 m/s and slice thickness ranging between 6 and 8 mm resulted in lower FRAP-Simulated intestinal digested value.

$$Y12\,(FRAP - Simulated\ intestinal\ digested) = 13.070 + 1.270X_1 + 0.430X_2 - 0.538X_3 - 2.330X_1X_2 + 2.390X_1X_3 - 0.145X_1^2 + 1.450X_2^2 + 0.525X_3^2 \quad (13)$$

Table 5 Criteria for optimization for process conditions

Response	Goal	Lower	Target	Experimental condition	Predicted condition
Y1	Maximize	233.51	719.07	587.65	642.06
Y2	Maximize	363.74	802.13	781.96	751.63
Y3	Maximize	375.23	618.84	568.45	597.57
Y4	Maximize	2.09	4.13	3.85	3.74
Y5	Maximize	2.05	5.15	4.95	5.25
Y6	Maximize	0.79	4.15	2.76	3.05
Y7	Maximize	3.60	8.07	5.87	5.66
Y8	Maximize	5.33	10.43	9.03	8.79
Y9	Maximize	1.19	3.97	3.75	4.56
Y10	Maximize	12.12	20.56	14.83	16.19
Y11	Maximize	13.08	35.92	35.19	33.94
Y12	Maximize	9.67	17.91	16.67	19.32
Composite desirability = 0.777					

Optimization of levels of independent variables

In order to optimize the levels of the independent variables (drying air temperature, drying air velocity and slice thickness) for drying melon slices having high quality, the responses (TPC– Undigested, TPC-Simulated gastric digestion, TPC-Simulated intestinal digestion, DPPH–Undigested, DPPH-Simulated gastric digestion, DPPH-Simulated intestinal digestion, CUPRAC–Undigested, CUPRAC-Simulated gastric digestion, CUPRAC-Simulated intestinal digestion, FRAP–Undigested, FRAP-Simulated gastric digestion, FRAP-Simulated intestinal digestion) were assigned equal importance on the basis of their effects on the quality of final product. The used criteria, actual and predicted responses were given in Table 5. The optimal condition for all responses with composite desirability of 0.777 was: 35 °C drying air temperature, 0.5 m/s drying air velocity and 9 mm slice thickness.

Conclusion

Since melon is a seasonal fruit, it is unavailable throughout the year. For this reason, dried melon slices could be produced as an innovative snack for health-conscious consumers. Heat pump drying stands as a promising technique for drying of melon slices at a low temperature compared to drying with conventional methods. Dried melon slices could be accepted as an innovative snack both for the functional foods manufacturers and health-conscious consumers. The optimal drying condition with composite desirability of 0.777 was: 35 °C air temperature, 0.5 m/s air velocity and 9 mm slice thickness. The melons dried under optimized conditions preserved their phenolics and antioxidant capacity with their higher bioavailability.

References

1. P.M. Rolim, L.M.J. Seabra, G.R. de Macedo, Food Rev. Int. **36**, 15 (2020)
2. M. Pitrat, *Vegetables I: Asteraceae, Brassicaceae, Chenopodicaceae, and Cucurbitaceae, edited by J Prohens and F. Nuez* (Springer, New York, NY, 2008), pp. 283–315
3. J.F. Fundo, F.A. Miller, E. Garcia, J.R. Santos, C.L.M. Silva, T.R.S. Brandão, Food Meas **12**, 292 (2018)
4. A.L. Amaro, A. Oliveira, D.P.F. Almeida, Processing and impact on active components, in *Food*. ed. by V. Preedy (Academic Press, San Diego, 2015), pp. 165–171
5. I. Henan, I. Tlili, T. R'him, A.B. Ali, H. Jebari, J. New Sci. **29**, 1672 (2016)
6. A. Chakraverty, A.S. Mujumdar, H.S. Ramaswamy, *Handbook of Postharvest Technology: Cereals, Fruits, Vegetables, Tea, and Spices* (CRC Press, Boca Raton, 2003)
7. I.A.M. Ahmed, F. Al Juhaimi, M.M. Özcan, N. Uslu, E.E. Babiker, K. Ghafoor, M.A. Osman, H.A.A. Salih, J. Food Process. Preserv. **45**, 5605 (2021)
8. B.E. Filiz, A.C. Seydim, J. Food Biochem. **42**, e12676 (2018)
9. G. Dias da Silva, Z.M.P. Barros, R.A.B. de Medeiros, C.B.O. de Carvalho, S.C. Rupert Brandão, P.M. Azoubel, LWT **74**, 114 (2016)
10. M. Sabovics, S. Ishiyazova, L. Tomsone, S. Kampuse, H. Tilavov, and T. Ostonakulov, Foodbalt. 154 (2019)
11. S. Kamiloglu, E. Capanoglu, Int. J. Food Sci. Technol. **48**, 2621 (2013)
12. S.P. Ong, *Advances in Heat Pump-Assisted Drying Technology* (CRC Press, Newyork/USA, 2016), pp. 149–173
13. Z. Erbay, F. Icier, Drying Technol. **27**, 416 (2009)
14. S.P. Ong, C.L. Law, Drying Technol. **29**, 429 (2011)
15. A.M. Preciado-Saldaña, J. Abraham Domínguez-Avila, J. Fernando Ayala-Zavala, M.A. Villegas-Ochoa, S.G. Sáyago-Ayerdi, A. Wall-Medrano, A. González-Córdova, G.A. González-Aguilar, Food Sci. Technol. Int. **25**, 547 (2019)
16. J. Liu, X. Li, Y. Yang, H. Wei, L. Xue, M. Zhao, J. Cai, Food Sci. Nutr. **9**, 4568 (2021)
17. Z. Šumić, A. Vakula, A. Tepić, J. Čakarević, J. Vitas, B. Pavlić, Food Chem. **203**, 465 (2016)
18. M.R. Islam Shishir, F.S. Taip, N.A.B. Aziz, R.A. Talib, M.D.S. Hossain Sarker, Food Sci. Biotechnol. **25**, 461 (2016)
19. F. Jafari, K. Movagharnejad, E. Sadeghi, Food Chem. **333**, 127423 (2020)
20. M.J. Dalvand, S.S. Mohtasebi, S. Rafiee, Food Sci. Nutr. **2**, 200 (2014)
21. I. Golpour, M. Kaveh, R. Amiri Chayjan, R.P.F. Guiné, Int. J. Fruit Sci. **20**, 115 (2020)
22. E. Taghinezhad, M. Kaveh, A. Szumny, Foods **10**, 284 (2021)
23. M.K. Gupta, V.K. Sehgal, S. Arora, J. Food Sci. Technol. **50**, 62 (2013)
24. H. Majdi, J.A. Esfahani, M. Mohebbi, Comput. Electron. Agric. **156**, 574 (2019)
25. C. Tunckal, A. Ozkan Karabacak, C.E. Tamer, P. Yolci Omeroglu, Z. Goksel, Lat. Am. Appl. Res. (2022).
26. G.J. McDougall, P. Dobson, P. Smith, A. Blake, D. Stewart, J. Agric. Food Chem. **53**, 5896 (2005)
27. S. Kamiloglu, M. Demirci, S. Selen, G. Toydemir, D. Boyacioglu, E. Capanoglu, J. Sci. Food Agric. **94**, 2225 (2014)
28. S. Kamiloglu, M. Tomas, T. Ozdal, E. Capanoglu, Trends in Food Sci. Technol. **117**, 15 (2021).
29. F.J. Barba, L.R.B. Mariutti, N. Bragagnolo, A.Z. Mercadante, G.V. Barbosa-Cánovas, V. Orlien, Trends Food Sci. Technol. **67**, 195 (2017)
30. M.M.-L. Grundy, C.H. Edwards, A.R. Mackie, M.J. Gidley, P.J. Butterworth, P.R. Ellis, Br. J. Nutr. **116**, 816 (2016)
31. S. Kayacan, S. Karasu, P.K. Akman, H. Goktas, I. Doymaz, O. Sagdic, LWT **118**, 1830 (2020)
32. C. Galanakis, Food Sci. Nutr. (2017). http://scitechconnect.elsevier.com/bioavailability-bioaccessibility-bioactivity-food-components/. Accessed 05 September 2021
33. E. A. Panagopoulou, A. Chiou, M. Bismpikis, P. Mouraka, E. Mangiorou, V.T. Karathanos, Int. J. Food Sci. Technol. **56**, 4506 (2021)
34. C. Tunckal, İ Doymaz, Renew. Energy **150**, 918 (2020)
35. S. Kamiloglu, E. Capanoglu, Int. J. Food Sci. Technol. **49**, 1027 (2014)
36. G.A. Spanos, R.E. Wrolstad, J. Agric. Food Chem. **38**, 1565 (1990)
37. V. Katalinic, M. Milos, T. Kulisic, M. Jukic, Food Chem. **94**, 550 (2006)
38. R. Apak, K. Güçlü, M. Özyürek, S.E. Çelik, Microchim. Acta **160**, 413 (2008)
39. I.F.F. Benzie, J.J. Strain, Anal. Biochem. **239**, 70 (1996)
40. M. Minekus, M. Alminger, P. Alvito, S. Ballance, T. Bohn, C. Bourlieu, F. Carrière, R. Boutrou, M. Corredig, D. Dupont, C. Dufour, L. Egger, M. Golding, S. Karakaya, B. Kirkhus, S.L. Feunteun, U. Lesmes, A. Macierzanka, A. Mackie, S. Marze, D.J. McClements, O. Ménard, I. Recio, C.N. Santos, R.P. Singh, G.E. Vegarud, M.S.J. Wickham, W. Weitschies, A. Brodkorb, Food Funct. **5**, 1113 (2014)
41. T. Bileva, N. Petkova, T. Babrikov, Bull. UASVM Food Sci. Technol. **77**, 17 (2020)
42. R. Gómez-García, D.A. Campos, C.N. Aguilar, A.R. Madureira, M. Pintado, Trends Food Sci. Technol. **99**, 507 (2020)
43. C. Manach, A. Scalbert, C. Morand, C. Rémésy, L. Jiménez, Am. J. Clin. Nutr. **79**, 727 (2004)
44. İ Gulcin, Arch. Toxicol. **94**, 651 (2020)
45. K.J. Hunter, J.M. Fletcher, Innov. Food Sci. Emerg. Technol. **3**, 399 (2002)
46. B. Guldiken, G. Toydemir, K. Nur Memis, S. Okur, D. Boyacioglu, E. Capanoglu, Int. J. Mol. Sci. **17**, 858 (2016)
47. M. Tomas, G. Toydemir, D. Boyacioglu, R.D. Hall, J. Beekwilder, E. Capanoglu, J. Sci. Food Agric. **97**, 3106 (2017)
48. H. Şelale, H.O. Sıgva, İ Celik, S. Doganlar, A. Frary, Int. J. Food Prop. **15**, 145 (2012)
49. I.A.M. Ahmed, F.A. Juhaimi, M.M. Özcan, N. Uslu, E.E. Babiker, K. Ghafoor, M.A. Osman, H.A.A. Salih, J. Food Process. Preserv. **45**, 5605 (2021)
50. A. Bhatt, V. Patel, Free Radic. Antioxid. **3**, 30 (2013)

51. V. Pavan, R.A.S. Sancho, G.M. Pastore, LWT—Food Sci. Technol. **59**, 1247 (2014)
52. J.I. Mosele, A. Macià, M.-P. Romero, M.-J. Motilva, Food Chem. **201**, 120 (2016)
53. B. Gullon, M.E. Pintado, J. Fernández-López, J.A. Pérez-Álvarez, M. Viuda-Martos, J. Funct. Foods **19**, 617 (2015)
54. R. Lucas-Gonzalez, S. Navarro-Coves, J.A. Pérez-Álvarez, J. Fernández-López, L.A. Muñoz, M. Viuda-Martos, Ind. Crops Prod. **94**, 774 (2016)
55. M. Tomas, J. Beekwilder, R.D. Hall, O. Sagdic, D. Boyacioglu, E. Capanoglu, Food Chem. **220**, 51 (2017)
56. J. Bouayed, L. Hoffmann, T. Bohn, Food Chem. **128**, 14 (2011)
57. J.A. Larrauri, P. Rupérez, F. Saura-Calixto, J. Agric. Food Chem. **45**, 1390 (1997)
58. A.A. Hamama, W.W. Nawar, J. Agric. Food Chem. **39**, 1063 (1991)
59. D.L. Luthria, S. Mukhopadhyay, J. Agric. Food Chem. **54**, 41 (2006)
60. M.Y. Coseteng, C.Y. Lee, J. Food Sci. **52**, 985 (1987)
61. Y. Song, Y. Yao, H. Zhai, Y. Du, F. Chen, W. Shu-wei, Agric. Sci. China **6**, 607 (2007)
62. W. Jin, M. Zhang, W. Shi, Drying Technol. **37**, 387 (2019)
63. Ö.A. Gümüşay, A.A. Borazan, N. Ercal, O. Demirkol, Food Chem. **173**, 156 (2015)
64. E. Capanoglu, Int. J. Food Prop. **17**, 690 (2014)
65. M.C. Nicoli, M. Anese, M. Parpinel, Trends Food Sci. Technol. **10**, 94 (1999)
66. M. Al-Farsi, C. Alasalvar, A. Morris, M. Baron, F. Shahidi, J. Agric. Food Chem. **53**, 7592 (2005)
67. C.-H. Chang, H.-Y. Lin, C.-Y. Chang, Y.-C. Liu, J. Food Eng. **77**, 478 (2006)
68. Z. Tan, F. Shahidi, Food Chem. **133**, 1427 (2012)
69. M. Lutz, J. Hernández, C. Henríquez, CyTA—J. Food **13**, 541 (2015)
70. S. Devahastin, C. Niamnuy, Int. J. Food Sci. Technol. **45**, 1755 (2010)
71. A. Vega-Gálvez, K. Ah-Hen, M. Chacana, J. Vergara, J. Martínez-Monzó, P. García-Segovia, R. Lemus-Mondaca, K. Di Scala, Food Chem. **132**, 51 (2012)
72. M. Miranda, A. Vega-Gálvez, J. López, G. Parada, M. Sanders, M. Aranda, E. Uribe, K. Di Scala, Ind. Crops Prod. **32**, 258 (2010)
73. I.O. Minatel, C.V. Borges, M.I. Ferreira, H.A.G. Gomez, C.Y.O. Chen, G.P.P. Lima, *Phenolic Compounds: Biological Activity* (BoD Books on Demand, Croatia, 2017), pp. 1–23
74. S. Kamiloglu, G. Ozkan, H. Isik, O. Horoz, J. Van Camp, E. Capanoglu, LWT **77**, 475 (2017)
75. A. Shrivastava, A.D. Tripathi, V. Paul, D. Chandra Rai, LWT **151**, 112091 (2021)